J. Austral. Math. Soc. Ser. B 30(1988), 157–178

ON THE FINITE DEAN PROBLEM: LINEAR THEORY

B. J. KACHOYAN[1] AND P. J. BLENNERHASSETT[2]

(Received 7 May 1987; revised 17 December 1987)

Abstract

The Dean problem of pressure-driven flow between finite-length concentric cylinders is considered. The outer cylinder is at rest and the small-gap approximation is used. In a similar procedure to that of Blennerhassett and Hall [8] in the context of Taylor vortices, special end conditions are imposed in which the ends of the cylinder move with the mean flow, allowing the use of a perturbation analysis from a known basic flow. Difficulties specific to Dean flow (and more generally to non-Taylor-vortex flow) require the use of a parameter α which measures the relative strengths of the velocities due to rotation and the pressure gradient, to trace the solution from Taylor to Dean flow. Asymptotic expansions are derived for axial wavenumbers at a given Taylor number. The calculation of critical Taylor number for a given cylinder height is then carried out. Corresponding stream-function contours clearly show features not evident in infinite flow.

1. Introduction

The centrifugal instability of flow between concentric cylinders has a rich history of detailed investigation. Nevertheless, most theoretical analyses have concentrated on cylinders which were assumed to be infinitely long, allowing classical Couette (or Poiseuille) flow to be an admissible solution. Experiments have indicated that, for most cylindrical lengths, the ends are important in determining the flow configuration (which may, or may not, be unique) and in fact may drive the transition to a secondary steady state (see, for example Snyder and Lambert [36], Burkhalter and Koschmieder [10], and the series of Benjamin [2], [3], [4] and Benjamin and Mullin [5] [6]). Clearly an understanding of the effects of imposing

[1]Department of Applied Mathematics, University of Sydney, Sydney, N.S.W. 2006, Australia.
[2]School of Mathematics, University of New South Wales, P. O. Box 1, Kensington, N.S.W., 2033, Australia.

a finite regime is desirable. When the cylinders are of finite length, however, and the end plates fixed, Couette (or Poiseuille) flow is no longer a solution to the Navier-Stokes equations, with conditions of no slip on the boundaries, and all velocity components must always have some dependence on the axial variable.

Thus, even at low Taylor numbers, there exists a slow axial circulation which develops smoothly into classical Taylor vortex flow rather than the bifurcation predicted for infinite cylinders. The experiments of Snyder and Lambert [36], Cole [14] and Pfister and Rehberg [30], for example, show observations of axial flows for $T < T_c$, and the numerical work of Alziary de Roquefort and Grillaud [1] shows similar behaviour. Smoothly developing cellular motion was also shown to exist experimentally in convection in a box by, for example, Bergé [7]. Benjamin [2] gave a qualitative theoretical discussion of the effects of a bounded domain in general flows with particular reference to Taylor vortex flow.

Analytical work on cylinders of finite extent began with Blennerhassett and Hall [8] who considered the narrow-gap linear stability problem for Taylor vortices with a stationary outer cylinder. Ends were imposed on the cylinders, which were assumed to move with the azimuthal velocity of the corresponding infinite flow. These artificial end conditions remove the smooth transitions which we have seen are normally associated with finite cylinders, and allow the use of perturbation analyses from a known mean flow (Couette flow in [8]). It is hoped that the essential features of finite-domain flow will be retained without the necessity of a fully numerical solution at all values of Taylor number.

The bifurcations in [8] may be converted to a more realistic smooth transition by introducing small imperfections to the boundary conditions; a similar phenomenon was found to occur in convection in a box by Hall and Walton [22] and Daniels [15]. See also Reiss [32] for a description of the effects of imperfections in buckling problems. An alternative was proposed by Schaeffer [34]. He introduced boundary conditions with an adjustable parameter β such that $\beta = 0$ corresponded to the conditions in [8] while $\beta = 1$ represented fixed ends. A perturbation for $\beta \neq 0$ but $\beta \ll 1$ from an analysis such as that of Hall [24] would then result in the smooth development of a flow which, it would be hoped, would be at least qualitatively the same as the true problem. This model is further discussed in Benjamin and Mullin [5], and used quantitatively by Hall in [23] and [24].

The critical Taylor number for instability is, of course, a function of cylinder height L. In [8], it was found that solutions, even and odd in the axial variable z, could be treated separately and lead to critical Taylor numbers, $T_{c_e}(L)$ and $T_{c_0}(L)$, respectively. Furthermore, the curves of T_{c_e} and T_{c_0} interlace. Similar results were found in the convection of a layer of fluid heated from below in a two-dimensional box (Drazin [20], Daniels [16]).

In this paper, we shall study the corresponding approach to the Dean problem [17] where the mean motion is pressure-driven Poiseuille flow. This type of flow is intended to model flow in curved rectangular pipes, and flow in helically coiled ducts with small pitch. Recent numerical and experimental work on this problem has been carried out by, for example, Winters [38], Hille et al. [25], Joseph et al. [27], Ghia and Sokhey [21], De Vriend [18] and Cheng et al. [13].

The linear analyses of this paper and [8] do not address themselves to the question of the stability of solutions which bifurcate from the azimuthal flow. Hence, any of the flow patterns described here are not necessarlty expected to eventuate, but are demonstrations of the variety of solutions made possible by a restriction of the domain. A weakly-nonlinear analysis will be given in a future paper (Kachoyan [28]) which will investigate the growth of steady solutions and which will include a comparison with the above previous work, especially that of Winters [38].

The structure of this paper is as follows. In Section 2 we derive the system of differential equations governing Taylor-Dean flow. Section 3 outlines the calculation and ordering of the complex axial wavenumbers and corresponding eigenfunctions needed to satisfy the end conditions. It is found that the wavenumbers for the Dean problem are difficult to find directly and need to be traced from the known Taylor-vortex results through the joint Taylor-Dean problem. For a given Taylor number, we find asymptotic expressions for large wavenumbers in Section 4. These expressions give a check on the numerical solutions. Moreover, they indicate that care should be taken with the method in [8] (essentially an extension of the Galerkin-type approach developed by Chandrasekhar [11], [12] when the critical eigenfunctions are either not well approximated by sinusoids, or have large high frequency components.

Section 5 describes the calculation of Taylor numbers T for instability at a given cylinder length L. The curves of Taylor number against cylinder length for solutions, even and odd in the axial variable z, are found to intertwine as in [8]. Flow patterns not seen in the infinite cylinder case were reported by Blennerhassett and Hall in [8] in their solution of the Taylor vortex problem. Streamfunction contours revealed nonplanar vortex boundaries as well as weak vortices near the ends of the cylinders and in the interior of the fluid. In addition, adjacent co-rotating vortices were found at various values of (L, T). In Section 6, similar phenomena are found in the present linear stability calculation. By considering the limit $L \to \infty$, Blennerhassett and Hall in [8] showed that the double-cell/weak-cell structures can be ascribed to a slow modulation of the main flow caused by the distant boundaries. Their analysis is equally valid in the Dean problem, and the asymptotic form of T at large L for the Dean problem is given in Section 6.

2. Formulation of equations

We consider a pair of concentric cylinders of inner radius R_1 and outer radius R_2 ($R_2 > R_1$) and suppose the ends of the cylinders to be at $z^* = \pm Ld$ where $d = R_2 - R_1$ and where we have used the cylindrical polar coordinates (r^*, θ, z^*) with the axis of the cylinders the z^*-axis. The corresponding velocity distributions will be given by (U^*, V^*, W^*). We shall make the small-gap approximation as in [8], so that

$$d \ll \frac{1}{2}(R_1 + R_2).$$

Motion is driven by the inner cylinder rotating with angular velocity Ω_1 and by imposing a pressure gradient $\partial P^*/\partial\theta = -\kappa\rho$, where ρ is the density of the fluid and κ is a constant. A pressure distribution of this form is clearly unable to be exactly realisable but is nevertheless a useful analytical approximation to experimental conditions.

In the case of infinite-length cylinders, this configuration admits steady axisymmetric flow with a velocity distribution of the form

$$U = 0, \quad V = V_0(x) = 2\alpha(1-x) + 6(1-\alpha)(x - x^2), \quad W = 0, \tag{2.1}$$

where

$$\alpha = V_T/(V_T + V_D), \quad V_T = \Omega_1 R_1/2 \quad \text{and} \quad V_D = \kappa d^2/(12\nu R_1).$$

Here ν is the kinematic viscosity, $x = (r^* - R_1)/d$ and the basic, steady azimuthal flow $V^*(r^*)$ has been scaled on $V_T + V_D$, the mean velocity around the cylinders.

For the stability calculation, we have scaled the velocities following Seminara and Hall [33], that is,

$$(U^*, V^*, W^*) = \left(\frac{\nu}{2d}U, (V_T + V_D)V, \frac{\nu}{2d}W\right). \tag{2.2}$$

Note that $\alpha = 1$ corresponds to Couette flow (which leads to Taylor vortices) whereas $\alpha = 0$ corresponds to Poiseuille flow (leading to Dean vortices) and is thus similar to the parameter N used by Brewster et al. [9]. DiPrima [19] used a parameter $Q = 3V_D/V_T$ in the present notation. The formulation of DiPrima, however, required the rescaling of the velocities in the Dean limit $Q \to \infty (V_T \to 0)$. The use of α obviates such rescaling. A description of the present formulation in the context of the infinite cylinder work of Brewster et al. [9], DiPrima [19] and others, is given in Kachoyan [29].

The perturbation to this basic solution is made such that

$$U = u(x, z, t), \quad V = V_0(x) + v(x, z, t), \quad W = w(x, z, t), \tag{2.3}$$

where the perturbations (u, v, w) are assumed small compared with the basic flow V_0. Neglecting products of the perturbation quantities and eliminating w

https://doi.org/10.1017/S0334270000006135 Published online by Cambridge University Press

using continuity, the resulting equations to be solved are

$$\left(\frac{\partial}{\partial t} - \nabla^2\right)\nabla^2 u - TV_0 v_{zz} = 0 \qquad \text{and} \qquad \left(\frac{\partial}{\partial t} - \nabla^2\right)v + \frac{1}{2}uV_0' = 0, \tag{2.4}$$

where $\nabla^2 = \partial^2/\partial x^2 + \partial^2/\partial z^2$ is the Laplacian. Subscripted variables mean partial differentiation, the dash refers to differentiation with respect to x, and T is the Taylor number:

$$T = 4(V_T + V_D)^2 d^3/(\nu^2 R_1). \tag{2.5}$$

In an infinite cylinder the fluid velocity is given by (2.1). In a real flow between cylinders of finite length, the velocity is approximately (2.1) away from the ends provided the Taylor number is below critical. We choose conditions on the ends $|z| = L$ so as to model the real flow by a purely azimuthal flow in $|z| \leq L$. There are several choices of end condition which achieve our aim but we follow the method in [8], and assume the ends of the cylinder are moving with the flow (2.1).

Thus we impose the conditions

$$U = 0, \quad V = V_0(x), \quad W = 0 \qquad \text{on } |z| = L,$$

and so by (2.3) the perturbations to the basic azimuthal flow must vanish at the ends. Hence we have the homogeneous conditions

$$u = v = w = 0 \qquad \text{on } x = 0, 1, \quad -L \leq z \leq L$$

and

$$u = v = w = 0 \qquad \text{on } z = \pm L, \quad 0 \leq x \leq 1. \tag{2.6}$$

The end conditions we have adopted could not be easily realised physically. However, we suggest that the purely azimuthal flow confined to $|z| = L$ is a reasonable model of the real flow, and that its stability can provide some insight to the experimental observations and numerical calculations on flows in finite length containers.

We now seek a separated solution of the form (see [8])

$$\begin{aligned} u &= u(x)\exp(ikz)\exp(i\sigma t) + \text{c.c.}, \\ v &= v(x)\exp(ikz)\exp(i\sigma t) + \text{c.c.}, \\ w &= w(x)\exp(ikz)\exp(i\sigma t) + \text{c.c.}, \end{aligned} \tag{2.7}$$

where c.c. denotes complex conjugate and $w(x) = ik^{-1}\,du/dx$ from continuity. Substituting these into (2.4) gives

$$(D^2 - k^2 - i\sigma)(D^2 - k^2)u - k^2 TV_0 v = 0,$$

and

$$(D^2 - k^2 - i\sigma)v - \tfrac{1}{2}uV_0' = 0,$$

https://doi.org/10.1017/S0334270000006135 Published online by Cambridge University Press

where $D = d/dx$. Since we are looking for neutrally stable disturbances, we set $\sigma = 0$ and arrive at

$$(D^2 - k^2)^2 u - k^2 T V_0 v = 0, \tag{2.8a}$$

and

$$(D^2 - k^2) v - \tfrac{1}{2} u V_0' = 0, \tag{2.8b}$$

with $u = Du = v = 0$ on $x = 0, 1$.

The properties of this eigenvalue problem are discussed in [8]. Notably, for T less than some critical value T_{c_∞}, there are no real eigenvalues k of (2.8), whereas for each $T > T_{c_\infty}$ there are at least two distinct ones which define the neutral curves of the infinite problem. For all values of T, however, there are an infinite number of eigensolutions of (2.8) with possibly complex eigenvalues, denoted by $\pm k_n$, $n = 1, 2, 3, \ldots$. Thus the general solution of (2.8) is a linear combination of all possible eigensolutions, and the imposition of boundary conditions (2.6) will determine the unknown constants in the general solution. Sections 3 and 4 discuss the properties of the eigenvalues k_n and in Section 5 the imposition of boundary conditions is carried out.

3. Calculation of axial wavenumbers

We employ the method of solution of Chandrasekhar [11] in order to use it for the finite-length calculations of Section 5. In that section, the considerable time saving over a direct numerical approach assumes greater significance.

Thus, expanding the azimuthal eigenfunction $v_n(x)$, which corresponds to the eigenvalues $\pm k_n$, in a Fourier sine series automatically satisfying the boundary conditions on v, we get

$$v_n(x) = \sum_{p=1}^{\infty} C_{pn} \sin p\pi x. \tag{3.1}$$

Using this series, (2.8a) is solved for the radial eigenfunction $u_n(x)$ and the u_n and v_n are then substituted into (2.8b). The resultant equation is multiplied by $\sin j\pi x$ for $j = 1, 2, \ldots$, and integrated from $x = 0$ to $x = 1$ to give an infinite system of equations of the form

$$A_n \overline{C}_n = 0, \tag{3.2}$$

where $\overline{C}_n$ is the vector $(\overline{C}_{1n}, \overline{C}_{2n}, \ldots)^T$. A_n is an infinite square matrix given explicitly by Kachoyan [29].

It should be noted here that certain elements of the matrix A_n have poles, which can be shown to be of order one, at $\Delta_n = 0$, and $\gamma_m = 0$, $m = 1, 2, 3, \ldots$ where $\Delta_n = \sinh^2 k_n - k_n^2$ and $\gamma_m^2 = m^2\pi^2 + k_n^2$, that is, at $\sinh k_n = \pm k_n$ and $k_n = m\pi i$, $m = 1, 2, 3, \ldots$. This point will be discussed further later.

https://doi.org/10.1017/S0334270000006135 Published online by Cambridge University Press

The system (3.2) has a non-zero solution only if $|A_n| = 0$, which gives an eigenvalue problem determining the k_n as functions of T. Since (2.8) is real, the k_n must be either real, purely imaginary, or occur in complex conjugate pairs. A comprehensive survey of k_n for the Taylor vortex problem has been given in [8]. They found that the eigenvalues k_{3n-2}, k_{3n-1}, k_{3n} (with $k_{3n-2} = \bar{k}_{3n-1}$ and $\mathrm{Re}(k_{3n}) = 0$) corresponded to azimuthal velocity eigenfunctions $v_{3n-2}(x), \ldots, v_{3n}(x)$ having $n-1$ zeros in $(0,1)$. Furthermore, these velocity fields are dominated by the $p = n$ term in the Fourier expansion (3.1). The Dean problem is not as straightforward. Firstly, Reid [31] and Seminara and Hall [33] have shown that the azimuthal velocity for neutrally stable modes has a zero in $(0,1)$. Thus, in general, the first three eigenfunctions $v_1(x), v_2(x), v_3(x)$, in contrast to the Taylor vortex case, have one zero in $(0,1)$ and are dominated by $p = 2$ in the expansion (3.1).

Secondly, there is no unique ordering of wavenumbers k_n according to which the Fourier coefficient C_{pn} is dominant in (3.1) until n becomes large (typically > 12). To select an ordering which would give accurate results for a small number of wavenumbers, we used the parameter α to trace the evolution of the wavenumbers from the Taylor-vortex problem ($\alpha = 1$) to the Dean problem ($\alpha = 0$). In this way it was found that the wavenumbers can be ordered in groups of three according to the pattern given above. That is, a complex conjugate pair of wavenumbers (with the possible exception of the first two wavenumbers, which may be real) followed by a purely imaginary one. Within the confines of this pattern, the separate sets of complex and purely imaginary wavenumbers are ordered according to magnitude. It is shown in Section 4 that large wavenumbers asymptotically follow this pattern.

The Fourier coefficients C_{pn} are found by back-substitution in (3.2) and using $C_{pn} = \overline{C}_{pn}\gamma_p^4$. At this stage, the C_{pn}, $p = 1, 2, \ldots$ are normalised with respect to the largest Fourier coefficient at each n. Note that it is not only the accuracy of the k_n which is affected by the order of truncation of the determinant $|A_n|$, but also the number of roots which can be found. For example, truncation of $|A_n|$ to fourth order is equivalent to considering the first four Fourier coefficients of $v(x)$ and so, in general, we are then only able to find the first twelve roots (wavenumbers) of $|A_n|$. As a result, we do not get uniform accuracy for the wavenumbers k_n: at a given truncation of $|A_n|$ the accuracy decreases as n increases. Similarly, at each wavenumber, their corresponding Fourier coefficients C_{pn} become progressively less accurate as p increases.

For the Dean problem, taking six terms in the series (3.1) for $v_n(x)$, we obtain at least three significant figures in the eighteen wavenumbers it is possible to find. Their corresponding Fourier coefficients then range from three significant figures at low wavenumbers to only one significant figure at high wavenumbers. It is expected that the final solution will be dominated by the first wavenumbers and

this will compensate for the loss of accuracy at higher wavenumbers. In all these results we gain, in general, one significant figure for each extra pair of terms used in (3.1).

It should be noted that the Taylor vortex problem is generally more accurate by one significant figure or more for a given truncation of (3.1). Presumably this is due to the abovementioned ordering of dominant Fourier coefficients present in Taylor vortices.

To verify that all roots of $|A_n|$ were found, the MSL subroutine ZCOUNT was used. This routine calculates the number of zeros minus the number of poles of a function in a user supplied closed contour (actually a polygon) in the complex plane. As the locations of the poles of $|A_n|$ were known, the number of zeros of $|A_n|$, in a given region, could be found. The computations with ZCOUNT confirmed that we had located all the required zeros of $|A_n|$.

TABLE 1. Wavenumbers k_n and the dominant Fourier coefficient (F.C.) of their respective azimuthal velocity fields for the Dean problem at $T = 6000$.

n	k_n	*F.C.*
1	2.780	2
2	5.471	2
3	$1.700i$	2
4	$5.038 + 7.931i$	1
5	$5.038 - 7.931i$	1
6	$7.832i$	3
7	$4.728 + 10.314i$	2
8	$4.728 - 10.314i$	2
9	$11.239i$	1
10	$4.478 + 13.683i$	3
11	$4.478 - 13.683i$	3
12	$13.738i$	2
13	$4.396 + 16.934i$	4
14	$4.396 - 16.934i$	4
15	$16.745i$	4
16	$4.162 + 20.561i$	5
17	$4.162 - 20.561i$	5
18	$19.863i$	6

Table 1 shows a list of wavenumbers for the Dean problem at $T = 6000$ along with their dominant Fourier coefficient in (3.1). A sample of wavenumbers and the Fourier coefficients of their velocity fields is shown in Table 2 for the Taylor vortex and Dean problems. These tables were calculated using six terms in (3.1).

https://doi.org/10.1017/S0334270000006135 Published online by Cambridge University Press

TABLE 2. Sample wavenumbers k_n and the Fourier coefficients C_{pn} of their respective azimuthal velocity fields, at typical values of the Taylor number for the Taylor vortex and Dean problems using six terms in (3.1).

	Taylor $\alpha = 1,\ T = 2000$		Dean $\alpha = 0,\ T = 6000$	
n	k_n	$C_{pn} \times 10^3$	k_n	$C_{pn} \times 10^3$
1	2.179	1000.	2.780	−674.2
		17.61		1000.
		−23.75		−104.9
		−0.879		−42.71
		−2.023		9.419
		−0.126		−7.750
3	$7.241i$	1000.	$1.700i$	817.7
		−553.5		1000.
		286.8		56.12
		−23.35		−41.07
		4.980		−4.944
		−0.870		−6.078
7	$3.248 + 9.501i$	$-75.52 - 125.8i$	$4.728 + 10.314i$	$246.0 - 689.3i$
		$-94.36 + 54.54i$		1000.
		1000.		$676.6 - 603.9i$
		$39.46 + 51.41i$		$67.75 + 87.10i$
		$-76.57 - 65.52i$		$-25.84 - 69.89i$
		$-0.85 - 1.75i$		$-18.50 - 10.32i$

The numerical results in this section were checked using a direct Runge-Kutta shooting approach to integrate numerically the governing differential equations. The Fourier coefficients of the eigenfunctions may then be checked using a Fast Fourier Transform algorithm (see, for example, Singleton [35]) with agreement at least to the significant figures quoted above being obtained.

4. Large wavenumber expansions at constant T

This section examines the behaviour of the eigenvalues k_n of (2.8) as $n \to \infty$ for constant T. In the previous section, it was seen that for $n > 3$, the k_n are either purely imaginary or come in complex conjugate pairs. Considering first the purely imaginary wavenumbers, we let $k = ik$ for convenience and write (2.8) as

$$(D^2 + k^2)^2 u = -k^2 T V_0(x) v, \qquad (D^2 + k^2) v = (1/2) u V_0'(x), \qquad (4.1)$$

where we recall that

$$u = Du = v = 0 \quad \text{on } x = 0, 1 \qquad \text{and} \qquad V_0(x) = 2\alpha(1 - x) + 6(1 - \alpha)(x - x^2).$$

We now fix T and look for solutions for large k. At this stage, there is no natural parameter for an expansion of k and no *a priori* information on the relationship between the size of k_n and n. To overcome these difficulties we

https://doi.org/10.1017/S0334270000006135 Published online by Cambridge University Press

introduce an artificial parameter κ, assumed large, and let

$$k = \kappa a, \qquad \text{where } a^2 = a_0^2 + \kappa^{-2}a_2 + \kappa^{-4}a_4 + \cdots . \tag{4.2}$$

The velocities are expanded as

$$v = A_0 \sin \kappa a_0 x + \kappa^{-1} A_1(x) \cos \kappa a_0 x + \kappa^{-2} A_2(x) \sin \kappa a_0 x + \dots ,$$

and

$$u = B_0(x) \sin \kappa a_0 x + \kappa^{-1} B_1(x) \cos \kappa a_0 x + \kappa^{-2} B_2(x) \sin \kappa a_0 x + \dots , \tag{4.3}$$

where A_0 is a constant and $B_0, A_1, B_1, \dots$ will be polynomials. Being free to normalise the velocities, we choose $A_0 = 1$ without loss of generality.

The boundary conditions on v immediately give us

$$\sin \kappa a_0 = 0, \qquad \text{or} \qquad \kappa a_0 = n\pi, \quad n = 1, 2, \dots . \tag{4.4}$$

Substituting the expansions (4.2) and (4.3) into the governing equations (4.1) we arrive at the following system of equations

$$-4B_0'' = -TV_0, \tag{4.5a}$$

$$-2A_1' a_0 = (1/2)V_0' B_0 - a_2, \tag{4.5b}$$

$$-4B_1'' a_0^2 + 4B_0''' a_0 = -Ta_0^2 V_0 A_1, \tag{4.5c}$$

$$2a_0 A_2' + A_1'' = (1/2)V_0' B_1, \tag{4.5d}$$

$$-4a_0^2 B_2'' = -V_0 T a_0^2 A_2, \tag{4.5e}$$

$$-2a_0 A_3' + A_2'' + a_4 = (1/2)V_0' B_2, \tag{4.5f}$$

with $A_1 = A_3 = B_0 = B_1 = B_1' + a_0 B_2 = 0$ at $x = 0, 1$.

Integrating (4.5a) and (4.5b) to find a_2 gives

$$B_0(x) = -(1-\alpha)(t/8)(x^4 - 2x^3 + x) - \alpha(T/12)(x^3 - 3x^2 + 2x),$$

and

$$\begin{aligned} -2a_0 A_1(x) = (T/48)[&(1-\alpha)^2(6x^6 - 18x^5 + 9x^4 + 12x^3 - 9x^2) \\ &+ \alpha(1-\alpha)(6x^5 - 24x^4 + 28x^3 - 9x^2) + \alpha^2(x^4 - 4x^3 + 4x^2)] - a_2 x \end{aligned}$$

where $A_1(1) = 0$ gives

$$a_2 = (T/48)(\alpha(1-\alpha) + \alpha^2) = \alpha T/48.$$

For the Dean problem, this term is identically zero and (4.5f) must be solved to find a_4. This integration is still quite straightforward, but rather tedious as the order of the polynomials involved increases rapidly, and the coefficients need to be determined exactly as there is much cancellation in the calculation of a_4. We thus make use of the algebraic manipulation package MACSYMA implemented on a VAX 11/750. The results were checked by hand for the Dean

problem up to and including $A_2(x)$. The polynomials for the Dean problem are given in Appendix A and the bounary conditions on $A_3(x)$ give

$$a_4 = 31T^2/(49280a_0^2).$$

Thus, for $\alpha \neq 0$,

$$k_{3n}^2 = n^2\pi^2 + \frac{\alpha T}{48} + \dots, \tag{4.6}$$

while for $\alpha = 0$,

$$k_{3n}^2 = n^2\pi^2 + \frac{31T^2}{49280}\frac{1}{n^2\pi^2} + \dots. \tag{4.7}$$

It can be seen from (4.6) and (4.7) that the first-order approximations to the purely imaginary k_n for large n are the poles of $|A_n|$ discussed in Section 3. For $\alpha \neq 0$, this is tempered by the next term in the series being $O(1)$. For $\alpha = 0$, problems may arise for large n, but due to the relatively large values of T (> 5000), they will not be expected to affect the numerical solution until $n \gg 10$.

Note also that this expansion confirms the ordering in [8], at least for large wavenumbers. That is, since for large n, $v_n(x) \sim \sin n\pi x$, the nth purely imaginary wavenumber will be dominated by the nth term in the Fourier expansion (3.1). A comparison of the results of Section 3 and the expansions (4.6) and (4.7) is given in Table 3 for $\alpha = 0, 1$.

TABLE 3. Comparison of values of wavenumber k_n at typical Taylor numbers with those given by the asymptotic expansions (4.6) and (4.7).

	Taylor $\alpha = 1,\ T = 2000$		Dean $\alpha = 0,\ T = 6000$	
n	k_{3n} (numerical)	k_{3n} (asymptotic)	k_{3n} (numerical)	k_{3n} (asymptotic)
2	$9.402i$	$9.008i$	$7.832i$	$24.761i$
4	$14.384i$	$14.127i$	$13.738i$	$11.975i$
6	$20.080i$	$19.924i$	$19.863i$	$20.470i$

We use similar expansions to (4.2) and (4.3) to find the complex wavenumbers k_{3n-1}, k_{3n-2}, $n = 2, 3, \dots$, namely

$$k = \kappa a, \quad a^2 = a_0^2 + \kappa^{-2}a_2 + \dots, \tag{4.8}$$

where now

$$u(x) = u_0(x) + \kappa^{-2}u_2(x) + \dots,$$
$$v(x) = \kappa^{-2}v_2(x) + \dots, \tag{4.9}$$

and the $a_0, a_2, \dots$ may be complex. Substituting (4.8) and (4.9) into (4.8) gives at leading order

$$(D^2 - \kappa^2 a_0^2)u_0 = 0, \tag{4.10}$$

https://doi.org/10.1017/S0334270000006135 Published online by Cambridge University Press

with $u_0 = Du_0 = 0$ at $x = 0, 1$, and where we have assumed $D \equiv d/dx$ to be of order κ. The eigenvalue problem (4.10) is the well-known Faddle-Papcovicz problem (see Hillman and Salzer [26]) which leads to the eigenrelation $\sinh^2 \kappa a_0 = (\kappa a_0)^2$. To first order, then, the eigenvalues k are the solutions of

$$\sinh k = k \qquad \text{and} \quad \sinh k = -k. \tag{4.11}$$

The nth solutions of (4.11), for n large, may in turn be written as

$$k_n = \log(4n + 1)\pi + i(2n\pi + \pi/2),$$

and

$$k_n = \log(4n - 1)\pi - i(2n\pi - \pi/2)$$

respectively.

From (4.11), the wavenumbers again asymptote to poles of $|A_n|$; however no difficulty was experienced in locating the required k_n from the zeros of $|A_n|$. In Table 4 we compare some results of Section 3 with the roots of (4.11).

TABLE 4. Comparison of values of wavenumber k_n obtained for the Dean problem at $T = 5162$ using twenty terms in (3.1) with the zeros, z_m^+ and z_m^- respectively, of $\sinh z = z$ and $\sinh z = -z$.

n	k_{3n-2}	m	z_m^+	z_m^-
2	$4.902 + 7.827i$	1	$2.769 + 7.498i$	
3	$4.522 + 10.355i$	2		$3.103 + 10.712i$
4	$4.326 + 13.676i$	2	$3.352 + 13.900i$	
5	$4.279 + 16.902i$	3		$3.551 + 17.073i$
19	$4.893 + 61.208i$	10		$4.810 + 61.183i$
20	$4.862 + 64.279i$	10	$4.860 + 64.327i$	

5. Calculation of T as a function of L

Having found the complex eigenvalues k_n of (2.8), we may write the neutrally stable solution as (cf. (2.7))

$$\begin{aligned} u(x, z) &= \sum_{n=1}^{\infty} \beta_n u_n(x) \exp(ik_n z) + \text{c.c.}, \\ v(x, z) &= \sum_{n=1}^{\infty} \beta_n v_n(x) \exp(ik_n z) + \text{c.c.}, \\ w(x, z) &= \sum_{n=1}^{\infty} \beta_n w_n(x) \exp(ik_n z) + \text{c.c.}, \end{aligned} \tag{5.1}$$

where the β_n are unknown constants.

https://doi.org/10.1017/S0334270000006135 Published online by Cambridge University Press

Due to the symmetry of the domain of the problem and the dependence on the square of the eigenvalues k^2 in (2.8), (5.1) can be separated into solutions which are either even or odd functions of z (u, v odd, w even and u, v even, w odd, respectively). A similar separation was made in [8] and can be made in several other stability problems in finite domains (see, for example, Drazin [20] for even and odd solutions to convection in a box). For the odd solutions, for example, we then write

$$\begin{aligned} u(x,z) &= \sum_{n=1}^{\infty} \beta_n u_n(x) \cos k_n z, \\ v(x,z) &= \sum_{n=1}^{\infty} \beta_n v_n(x) \cos k_n z, \\ w(x,z) &= -\sum_{n=1}^{\infty} \beta_n w_n(x) \sin k_n z, \end{aligned} \tag{5.2}$$

with $w_n(x) = k_n^{-1} du_n/dx$ from continuity.

Solutions with w odd in z (corresponding to an even number of vortices) are those which have been generally associated with Taylor vortex experiments, although more recently, even solutions have been observed (see, for example, Benjamin [3]). Note that Stuart and DiPrima [37] called the even solutions those whose radial and azimuthal velocity components are even in z; that is, u, v even and w odd in z.

It remains now to satisfy the boundary conditions (2.5) at the ends, $z = \pm L$. From (5.2) these give

$$\begin{aligned} \sum_{n=1}^{\infty} \beta_n u_n(x) \cos k_n L &= 0, \\ \sum_{n=1}^{\infty} \beta_n v_n(x) \cos k_n L &= 0, \\ -\sum_{n=1}^{\infty} \beta_n k_n^{-1} u_n'(x) \sin k_n L &= 0, \end{aligned} \tag{5.3}$$

for all x in $(0, 1)$, where $v_n(x)$ is given by (3.1) and $u_n(x)$ by (3.2).

Following [8], (5.3) is to be satisfied in a Galerkin sense. We thus multiply (5.3) by $\sin j\pi x$ for $j = 1, 2, \ldots$ and integrate from $x = 0$ to $x = 1$ to give an infinite set of equations of the form

$$\mathbf{B}\beta = 0, \tag{5.4}$$

https://doi.org/10.1017/S0334270000006135 Published online by Cambridge University Press

where $\beta = (\beta_1, \beta_2, \dots)^T$, and $\mathbf{B}$ is an infinite square matrix whose elements in the nth column and $3j-2$, $3j-1$, $3j$th rows are

$$\begin{aligned} B_{3j-2,n} &= \cos(k_n L) \int_0^1 u_n \sin j\pi x \, dx \\ B_{3j-1,n} &= \cos(k_n L) \int_0^1 v_n \sin j\pi x \, dx, \\ B_{3j,n} &= -\sin(k_n L) k_n^{-1} \int_0^1 u_n' \sin j\pi x \, dx \\ &= -\sin(k_n L) k_n^{-1} \frac{1}{j\pi} \int_0^1 u_n \cos j\pi x \, dx. \end{aligned} \tag{5.5}$$

The terms in (5.5) are given explicitly in Appendix B.

For the even solution, $\mathbf{B}$ is as above, but with $\cos(k_n L)$ replaced by $\sin(k_n L)$ and $-\sin(k_n L)$ replaced by $\cos(k_n L)$.

Ensuring that (5.4) has a nonzero solution requires

$$|\mathbf{B}| = 0 \tag{5.6}$$

which serves as an eigenvalue relation of the form $f(T, L) = 0$. It is numerically more economical to fix T, obtaining the k_n using the solvability condition on (3.2), and then find the value of L which satisfies (5.6). Backsubstitution in (5.4) enables us to find β which in turn determines the velocity fields $u(x, z)$, $v(x, z)$, $w(x, z)$ and the corresponding streamfunctions. The eigenvectors β are normalised such that $\beta_1 = 1$ and the eigenfunctions normalised such that the largest Fourier coefficient in (3.1) is 1.

6. Results and discussion

By truncating the series (3.1) for $v_n(x)$ at $p = N$ say, we restrict ourselves to $3N$ wavenumbers and (5.6) will involve the zeros of a $3N \times 3N$ determinant. It is found that $N = 4$ is sufficient to give at least three significant figures in the value of L for the Taylor problem and two for the Dean problem. One significant figure is gained, in general, for every subsequent pair of terms in (3.1) used. The curves of T against L were obtained by choosing a value of T, and then stepping through the values of L until a zero of $|\mathbf{B}|$ was bracketed. Müller's algorithm was then applied with termination when the root was known to a relative error of 10^{-8}. We may continue to step through the values of L at this stage enabling us to calculate simultaneously higher modes at a given Taylor number. The T vs L results obtained, as outlined above, were compared with results based on eigensolutions of (2.8) found by direct numerical solution. In all cases good agreement between the results of the two methods was obtained.

https://doi.org/10.1017/S0334270000006135 Published online by Cambridge University Press

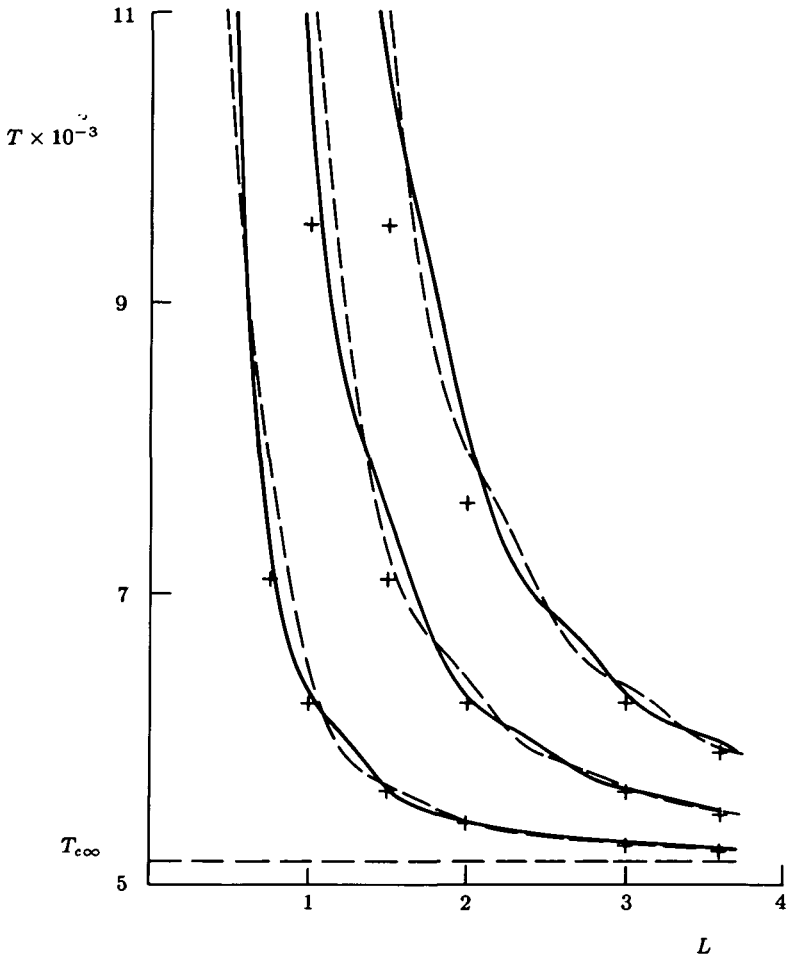

FIGURE 1. Critical Taylor numbers for the first three even and odd modes: ——— odd mode; — — even mode; + asymptotic solution.

We note in passing that the Fourier series method was about 40 times faster than the direct numerical method. The results of our calculations for the Taylor vortex problem were also checked against the results in [8], with agreement to the accuracy stated above. Figure 1 shows the curves of T against L for the first three even and odd modes for the Dean problem $\alpha = 0$. These neutral curves show interlacing similar to the Taylor vortex solutions.

In the limit $L \to \infty$, Blennerhassett and Hall [8] found T could be expanded as

$$T = T_{c\infty} + T_1 L^{-2} + \dots , \tag{6.1}$$

https://doi.org/10.1017/S0334270000006135 Published online by Cambridge University Press

with

$$T_1 = \tfrac{1}{2}\omega^2[d^2T/dk^2]_{k=k_{c\infty}}, \tag{6.2}$$

and

$$\omega^2 = (1/4)M^2\pi^2, \qquad M = 1, 2, 3, \ldots \tag{6.3}$$

where $(k_{c\infty}, T_{c\infty})$ is the minimum point on the neutral curve (see, for example, Kachoyan [29] or Seminara and Hall [33]). The corresponding axial velocities in the interior of the region are, at first order, proportional to terms such as, for the odd mode and $M = 2n-1$, $n = 1, 2, 3, \ldots$, $\sin(k_{c\infty}z)\cos(\frac{1}{2}M\pi z/L)$.

Evaluating (6.2) numerically for the Dean problem we obtain

$$T = 5161.8 + 1095.8M^2L^{-2} + \ldots, \qquad M = 1, 2, \ldots \tag{6.4}$$

Values of T for various values of L using (6.4) are also plotted in Figure 1.

TABLE 5. Typical values of $\beta_n \cos(k_n L)$ for the Dean problem. $T = 5600$, $L = 1.597$. Numbers in brackets denote multiplication by those powers of 10. These results are for the odd solution.

n	$\beta_n \cos(k_n L)$
1	0.1766
2	−0.1792
3	0.1177
4	−8.036(−2) + 7.945(−2)i
5	−8.036(−2) − 7.945(−2)i
6	−1.578(−2)
7	2.772(−3) + 1.337(−2)i
8	2.772(−3) − 1.337(−2)i
9	2.870(−2)
10	1.193(−2) + 6.971(−3)i
11	1.193(−2) − 6.971(−3)i
12	−2.136(−2)
13	1.235(−3) − 6.445(−3)i
14	1.235(−3) + 6.445(−3)i
15	9.904(−4)
16	5.332(−4) − 9.634(−5)i
17	5.332(−4) + 9.634(−5)i
18	2.003(−3)

Sample values of the eigenvectors β are shown in Table 5. The accuracy of each β_n decreases as n increases, in some cases dramatically. In fact, when using six terms in (3.1), β_{18} say, is in general only order of magnitude correct. The first few β_n's, however, (about 9) are correct to three significant figures and it is expected that these will dominate the expansion (5.1). We note that the decay $\beta_n \to 0$ as $n \to \infty$ is much more pronounced in Taylor vortex flow than Dean flow.

Notwithstanding the above difficulties, it was possible to obtain the stream-function to $2-3$ significant figures using six terms in (3.1). As found previously,

https://doi.org/10.1017/S0334270000006135 Published online by Cambridge University Press

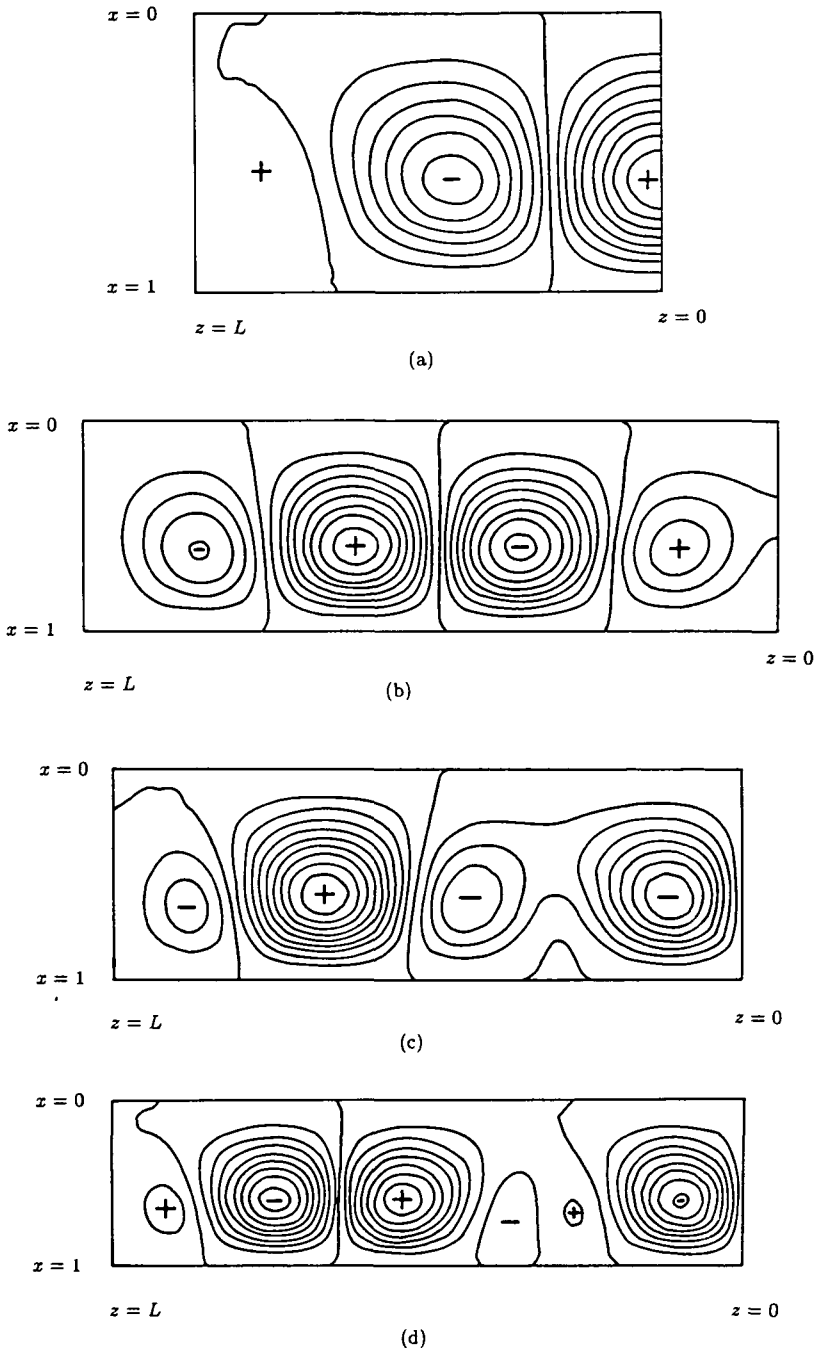

FIGURE 2. Streamfunction contours for (a) first even mode, $T = 5600$, $L = 1.681$; (b) second even mode, $T = 5600$, $L = 3.188$; (c) third odd mode, $T = 6600$, $L = 2.783$; (d) third odd mode, $T = 6000$, $L = 3.582$.

https://doi.org/10.1017/S0334270000006135 Published online by Cambridge University Press

one figure is gained per extra pair of terms in (3.1) used. Some streamfunction contours for the finite Dean problem are shown in Figure 2. In the case of infinite cylinders, the axial velocity is proportional to $\cos(k_{c_\infty} z)$, say, and hence the cell boundaries are equally spaced planes z =constant. The nature of the eigenvalues of (2.8) and the form of the solution (5.1) clearly shows that we cannot expect planar cell boundaries for the flow in the finite domain. Indeed Figure 2 shows that the cell boundaries can be quite convoluted. Figure 2a is typical of the streamfunction pattern obtained along the lowest even mode neutral curve in Figure 1. The streamfunction pattern for the lowest odd mode disturbance is similar to that of Figure 2a, but of course the plane $z = 0$ is now a cell boundary. As L becomes large, the cells away from the ends of the cylinder become more uniform in size, with cell boundaries becoming closer to planes of the form z =constant, i.e. the flow pattern is becoming more like that associated with infinite cylinders. In fact for every large L, the axial velocity has the form $\cos(\pi z/2L)\cos(k_{c_\infty} z) + o(1)$ for the lowest even mode, and $\cos(\pi z/2L)\sin(k_{c_\infty} z) + o(1)$ for the lowest odd mode, as in [8]. The weak end cells in Figure 2a appear to be the mechanism by which the number of cells in the flow changes as the length is increased. Increasing L from the value appropriate to Figure 2a causes the end cell to increase in strength and size until it is roughly the same size as the cells in the interior of the flow. Further increases in L cause the birth of a new weak cell at the ends, with this new cell usually appearing in the corners.

The higher neutral curves are a feature not present in the infinite cylinder case. Figures 2b, c and d show streamfunction contours for some higher modes and it is seen that quite different flow patterns are possible. A "double cell" is shown in Figure 2c and in Figure 2d there is a "weak cell" away from the ends of the cylinder. The origin of these structures is best explained in terms of the large L limit as in [8]. In this limit the axial velocity, say, has the form

$$\left.\begin{matrix}\cos((2n+1)\pi z/2L)\\ \sin(n\pi z/L)\end{matrix}\right\} \times \left\{\begin{matrix}\cos(k_{c_\infty} z)\\ \sin(k_{c_\infty} z)\end{matrix}\right. \quad \text{or}$$

The weak cell and double cell structures are produced by the interaction of the zeros of the modulation and the zeros of the infinite cylinder solution (see [8] for further details).

Experimental observations and computations on the finite Dean problem indicate that flow patterns corresponding to the higher modes described above are not observed. This is also true of the Taylor problem. However, weak end cells and flows with an odd number of vortices have been observed in the Taylor experiments (Benjamin [3]) and we suspect that they could exist for the Dean problem.

Of our results, it is the lowest-mode neutral curve which is important for comparison with experiment. It is this curve which defines the Taylor number T_c at which a purely azimuthal flow first becomes unstable to perturbations with a vortex structure. In an experiment, where the ends of the cylinder are stationary rigid boundaries, any vortices present for $T < T_c$ will be confined mainly to the ends, driven by the imbalance in centripetal pressure gradients. Over most of the length of the cylinder the flow will be approximately azimuthal. For T slightly greater than T_c, we predict that the whole length of the cylinder will be filled with vortices. A nonlinear analysis is required to predict the strength of the resultant vortices for $T > T_c$. The higher modes in this linear theory may then have some effect on secondary bifurcations from the vortex flow. However, it is our conjecture that flow patterns as in Figure 2c, d would all be unstable, and hence not experimentally observable.

The nonlinear analysis for the resultant vortex flow is presented elsewhere (Kachoyan [28]). We note that the critical Taylor numbers T_c found here are consistent with the results of Winters [38], who solved the full equations numerically. Winters also used bifurcation detection and continuation methods to follow the solution branches as the parameters were changed, and the results of Kachoyan [28] agree qualitatively with the numerical work of Winters. This and other aspects of the nonlinear problem are discussed in detail in Kachoyan [28].

Acknowledgement

The majority of this work was supported by the Commonwealth Postgraduate Awards Scheme at the University of New South Wales.

Appendix A

The polynomials of Section 4 are

$$B_1(x) = \frac{T}{8a_0}\left[\left(2+\frac{31T}{6720}\right)x - 6x^2 + 4x^3 + \frac{3T}{8}\left(-\frac{3}{20}x^5 + \frac{7}{30}x^6 - \frac{x^7}{42} - \frac{9}{56}x^8 + \frac{x^9}{9} - \frac{x^{10}}{45}\right)\right]$$

$$a_0^2 A_2(x) = \frac{T}{16}\left[-\frac{3}{2}x - \frac{31Tx^2}{4480} + \left(13+\frac{31T}{3360}\right)x^3 - \frac{39}{2}x^4 + \frac{39}{5}x^5 + \frac{3T}{8}\left(\frac{3}{40}x^6 - \frac{8}{35}x^7 + \frac{103}{560}x^8 + \frac{19}{504}x^9 - \frac{109}{840}x^{10} + \frac{x11}{15} - \frac{x^{12}}{90}\right)\right]$$

https://doi.org/10.1017/S0334270000006135 Published online by Cambridge University Press

$$a_0^2 B_2(x) = -\frac{T^3x^{16}}{614400} + \frac{T^3x^{15}}{76800} - \frac{99T^3x^{14}}{2609152} + \frac{211T^3x^{13}}{5591040} + \frac{67T^3x^{12}}{1720320} - \frac{27T^3x^{11}}{104800} + \frac{17T^3x^{10}}{143360} - \frac{3T^3x^9}{81920} + \frac{13T^2x^9}{1280} - \frac{117T^2x^8}{2560} + \frac{31T^3x^7}{1505280} + \frac{65T^2x^7}{896} - \frac{31T^3x^6}{614400} - \frac{13T^2x^6}{320} + \frac{93T^3x^5}{2867200} - \frac{9T^2x^5}{1280} + \frac{3T^2x^4}{256} - \frac{317T^3x}{111820800} + \frac{T^2x}{10752} - \frac{31T^2}{53760} - \frac{T}{4}$$

$$-2a_0^3 A_3(x) = -\frac{T^3x^{18}}{1843200} + \frac{T^3x^{17}}{204800} - \frac{8699T^3x^{16}}{521830400} + \frac{4439T^3x^{15}}{195686400} + \frac{449T^3x^{14}}{52183040} - \frac{2603T^3x^{13}}{37273600} + \frac{529T^3x^{12}}{5734400} - \frac{3T^3x^{11}}{57344} + \frac{61T^2x^{11}}{7040} + \frac{9T^3x^{10}}{819200} - \frac{61T^2x^{10}}{1280} + \frac{31T^3x^9}{2257920} + \frac{361T^2x^9}{3840} - \frac{1829T^3x^8}{40140800} - \frac{21T^2x^8}{320} + \frac{31T^3x^7}{627200} - \frac{207T^2x^7}{8960} - \frac{93T^3x^6}{5734400} + \frac{27T^2x^6}{512} - \frac{9T^2x^5}{512} - \frac{39Tx^4}{16} - \frac{317T^3x^3}{55910400} + \frac{T^2x^3}{5376} + \frac{39T^3}{8} + \frac{317T^3x^2}{74547200} - \frac{129T^2x^2}{35840} - \frac{51Tx^2}{16} + \frac{93T^2x}{35840} + \frac{3Tx}{4}$$

Appendix B

The elements in the nth column and $3j-2$, $3j-1$, $3j$th rows of the matrix B in (5.5) are given by

$$B_{3j-2,n} = Tk_n^2 \cos k_n L \sum_{p=1}^{\infty} \overline{C}_{pn}\{K^{pj} k_n [A_2^{(p)}(-1)^{n+1} \sinh k_n + B_2^{(p)}(1 + (-1)^{j+1} \cosh k_n)] - \psi_{pj}\},$$

$$B_{3j-1,n} = C_{jn} \cos k_n L,$$

$$B_{3j,n} = Tk \sin k_n L \sum_{p=1}^{\infty} \overline{C}_{pn}\{K_{pj} k_n^2 [A_2^{(p)}(1 + (-1)^{j+1} \cosh k_n) + B_2^{(p)}(-1)^{j+1} \sinh k_n] - \phi_{pj}\},$$

https://doi.org/10.1017/S0334270000006135 Published online by Cambridge University Press

where

$$\psi_{pj} = \begin{cases} \frac{-8pj\pi^2}{\gamma_j^2\gamma_p^2} - \frac{4pj}{p^2-j^2}\left(\frac{1}{\pi^2(p^2-j^2)} + \frac{2}{\gamma_p^2}\right) & p+j \text{ even},\ p \neq j, \\ \frac{1}{12} + \frac{1}{4p^2\pi^2} + \frac{4p^2\pi^2}{\gamma_p^4} & p = j, \\ 0 & p+j \text{ odd}; \end{cases}$$

$$\phi_{pj} = \begin{cases} 0 & p+j \text{ even}, \\ \frac{8pj\pi^2\gamma_p}{\gamma^2\gamma_p^2} - \frac{4pj}{(p^2-j^2)}\left[\frac{6(p^2\pi^2-k_n^2)}{\gamma_p^4} + \frac{p^2+3j^2}{\pi^2(p^2-j^2)^2} + \frac{8_p^2}{(p^2-j^2)\gamma_p^2}\right] & p+j \text{ odd}; \end{cases}$$

$$K_{pj} = \frac{P8pj\pi^2}{\gamma_j^4\gamma_p^2},$$

and all other quantities are as given by Kachoyan [29] with $\alpha = 0$.

References

[1] T. Alziary de Roquefort and G. Grillaud, "Computation of Taylor vortex flow in finite cylinders: linear theory", *Comput. & Fluids* **6** (1978) 259–269.

[2] T. B. Benjamin, "Bifurcation phenomena in steady flows of a viscous fluid. I. Theory", *Proc. Roy. Soc. London Ser. A* **359** (1978) 1–26.

[3] T. B. Benjamin, "Bifurcation phenomena in steady flows of a viscous fluid. II. Experiments", *Proc. Roy. Soc. London Ser. A* **359** (1978) 27–43.

[4] T. B. Benjamin, "New observations in the Taylor experiment." in *Transition and Turbulence.* (ed. R. E. Meyer). (Academic Press, 1981)

[5] T. B. Benjamin and T. Mullin, "Anomalous modes in the Taylor experiment", *Proc. Roy. Soc. London Ser. A* **377** (1981) 221–249.

[6] T. B. Benjamin and T. Mullin, "Notes on the multiplicity of flows in the Taylor experiment", *J. Fluid Mech.* **121** (1982) 219–230.

[7] P. Bergé, Rayleigh-Bénard instability: experimental findings obtained by light scattering and other optical methods. in *Fluctuations, Instabilities and Phase Transitions.* (ed. T. Riste). (Plenum Press, 1975)

[8] P. J. Blennerhassett and P. Hall, "Centrifugal instabilities of circumferential flows in finite cylinders: linear theory", *Proc. Roy. Soc. London Ser. A* **365** (1979) 191–207.

[9] D. B. Brewster, P. Grosberg and A. H. Nissan, "The stability of viscous flow between horizontal concentric cylinders", *Proc. Roy. Soc. London Ser. A* **251** (1959) 76–91.

[10] J. E. Burkhalter and E. L. Koschmieder, "Steady supercritical Taylor vortices after sudden starts", *Phys. Fluids* **17** (1974) 1929–1935.

[11] S. Chandrasekhar, "The stability of viscous flow between rotating cylinders", *Mathematika* **1** (1954) 5–13.

[12] S. Chandrasekhar, *Hydrodynamic and hydromagnetic stability* (Oxford University Press, 1961)

[13] K. C. Cheng, R.-C. Line, and J.-W. Ou, "Fully developed laminar flow in curved rectangular channels", *Trans. ASME J. Fluids Eng.* **98** (1976) 41–48.

[14] J. A. Cole, "Taylor vortices with short rotating cylinders", *Trans. ASME J. Fluids Eng.* **96** (1974) 69–70.

[15] P. G. Daniels, "Asymptotic sidewall effects in rotating Bénard convection", *Z. Angew. Math. Phys.* **28** (1977) 577–584.
[16] P. G. Daniels, "The effect of distant sidewalls on the transition to finite amplitude Bénard convection", *Proc. Roy. Soc. London Ser. A* **358** (1977) 173–197.
[17] W. R. Dean, "Fluid motion in a curved channel", *Proc. Roy. Soc. London Ser. A* **121** (1928) 402–420.
[18] J. H. De Vriend, "Velocity redistribution in curved rectangular channels", *J. Fluid Mech.* **107** (1981) 423–439.
[19] R. C. DiPrima, "The stability of viscous flow between rotating concentric cylinders with a pressure gradient acting round the cylinders", *J. Fluid Mech.* **6** (1959) 462–468.
[20] P. G. Drazin, "On the effects of sidewalls on Bénard convection", *Z. Angew. Math. Phys.* **26** (1975) 239–243.
[21] K. N. Ghia and J. S. Sokhey, "Laminar incompressible viscous flow in ducts of regular cross-section", *Trans. ASME J. Fluids Eng.* **99** (1977) 640–648.
[22] P. Hall and I. C. Walton, "The smooth transition to a convective régime in a two-dimensional box", *Proc. Roy. Soc. London Ser. A* **358** (1977) 199–221.
[23] P. Hall, "Centrifugal instabilities in finite containers: a periodic model", *J. Fluid Mech.* **99** (1980) 575–596.
[24] P. Hall, "Centrifugal instabilities of circumferential flows in finite cylinders: the wide gap problem", *Proc. Roy. Soc. London Ser. A* **384** (1982) 359–379.
[25] P. Hille, R. Vehrenkamp and E. O. Schultz-Dubois, "The development and structure of primary and secondary flow in a curved square duct", *J. Fluid Mech.* **151** (1985) 219–241.
[26] A. P. Hillmand and H. E. Salzer, "Roots of $\sin z = z$", *Phil. Mag.* **34** (1943) 575.
[27] B. Joseph, E. P. Smith and R. J. Adler, "Numerical treatment of laminar flow in a helically coiled tube of finit pitch", *Chem. Eng. Comm.* **7** (1975) 57–78.
[28] B. J. Kachoyan, "The finite Dean problem: nonlinear theory", *IMA J. Appl. Math* **38** (1987) 71–86.
[29] B. J. Kachoyan, "Neutral curve behaviour in Taylor-Dean flow", *Z. Angew. Math. Phys.* **38** (1987) 905–924.
[30] G. Pfister and I. Rehberg, "Space-dependent order parameter in circular Couette flow", *Phys. Lett. A* **83** (1981) 19–22.
[31] W. H. Reid, "On the stability of viscous flow in a curved channel", *Proc. Roy. Soc. London Ser. A* **244** (1958) 186–198.
[32] E. L. Reiss, "Imperfect bifurcation," in *Applications of Bifurcation Theory*, (ed. P. H. Rabinowitz), (Academic Press, New York, 1977), 37–71.
[33] G. Seminara and P. Hall, "Linear stability of slowly varying unsteady flows in a curved channel", *Proc. Roy. Soc. London Ser. A* **346** (1975) 279–303.
[34] E. H. Schaeffer, "Qualitative analysis of a model for boundary effects in the Taylor problem", *Math. Poc. Camb. Phil. Soc.* **87** (1980) 307–337.
[35] R. C. Singelton, "On computing the fast Fourier transform", *Comm. ACM* **10** (10) (1967) 647–654.
[36] H. A. Snyder and R. B. Lambert, "Harmonic generation in Taylor vortices between rotating cylinders", *J. Fluid Mech.* **26** (1966) 546–562.
[37] J. T. Stuart and R. C. DiPrima, "On the mathematics of Taylor vortex flows in cylinders of finite length", *Proc. Roy. Soc. Lond. Ser. A* **372** (1980) 357–365.
[38] K. H. Winters, "A bifurcation study of laminar flow in a curved tube of rectangular cross-section", *Harwell Report AERE TP.*1104. (1984)